
Rethinking Impersonation and Dodging Attacks on Face Recognition Systems

Fengfan Zhou¹, Qianyu Zhou², Bangjie Yin³, Hui Zheng³,
Xuequan Lu⁴, Lizhuang Ma², Hefei Ling^{1*}

¹Huazhong University of Science and Technology; ²Shanghai Jiao Tong University

³Shanghai Shizhuang Information Technology Co., Ltd; ⁴La Trobe University

¹{ffzhou, lhefei}@hust.edu.cn, ²zhouqianyu@sjtu.edu.cn, ²ma-lz@cs.sjtu.edu.cn
³jamesyin10@gmail.com, ⁴b.lu@latrobe.edu.au

Abstract

Face Recognition (FR) systems can be easily deceived by adversarial examples that manipulate benign face images through imperceptible perturbations. Adversarial attacks on FR encompass two types: impersonation (targeted) attacks and dodging (untargeted) attacks. Previous methods often achieve a successful impersonation attack on FR; However, it does not necessarily guarantee a successful dodging attack on FR in the black-box setting. In this paper, our key insight is that the generation of adversarial examples should perform both impersonation and dodging attacks simultaneously. To this end, we propose a novel attack method termed as Adversarial Pruning (Adv-Pruning), to fine-tune existing adversarial examples to enhance their dodging capabilities while preserving their impersonation capabilities. Adv-Pruning consists of Priming, Pruning, and Restoration stages. Concretely, we propose Adversarial Priority Quantification to measure the region-wise priority of original adversarial perturbations, identifying and releasing those with minimal impact on absolute model output variances. Then, Biased Gradient Adaptation is presented to adapt the adversarial examples to traverse the decision boundaries of both the attacker and victim by adding perturbations favoring dodging attacks on the vacated regions, preserving the prioritized features of the original perturbations while boosting dodging performance. As a result, we can maintain the impersonation capabilities of original adversarial examples while effectively enhancing dodging capabilities. Comprehensive experiments demonstrate the superiority of our method compared with state-of-the-art adversarial attacks.

1 Introduction

Thanks to the ceaseless advancements in deep learning, Face Recognition (FR) has achieved exceptional performance [41; 49; 9; 1; 2; 26]. However, the vulnerability of existing FR models to adversarial attacks poses a significant threat to their security. Hence, there is an urgent need to enhance the performance of adversarial face examples to expose more blind spots in FR models. As a result, several research endeavors have been directed towards this realm. A multitude of adversarial attacks have been developed to create adversarial face examples with characteristics such as stealthiness [40; 62; 7; 19; 42], transferability [70; 29; 72; 71], and physical attack capability [64; 63; 28]. These efforts contribute to enhancing the effectiveness of adversarial attacks on FR. Nevertheless, these studies primarily concentrate on bolstering either impersonation attacks or dodging attacks, overlooking the exploration of the effectiveness of dodging attacks when crafting adversarial face examples using impersonation attacks.

*Corresponding author

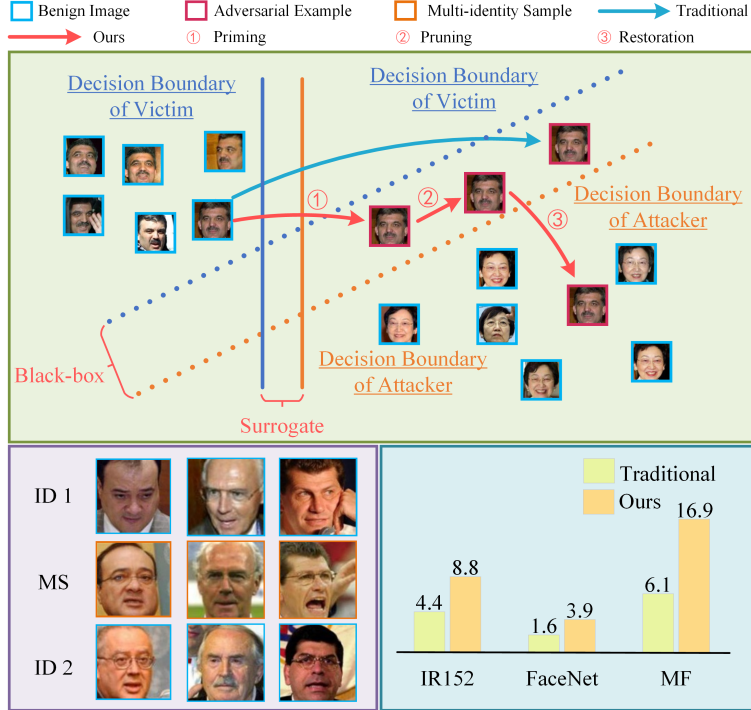


Figure 1: **Top:** previous methods that achieve a successful impersonation attack on FR cannot guarantee a successful dodging attack on FR in the black-box setting. In contrast, we present Adv-Pruning, including Priming, Pruning, and Restoration Stages, to perform both impersonation and dodging attacks simultaneously. **Bottom (left):** natural Multi-identity Samples (MS). **Bottom (right):** the dodging Attack Success Rate (%) between the previous methods and Adv-Pruning on multiple models.

In real-world deployment contexts, individuals with malicious intent are prone to creating adversarial face examples incorporating their own facial features to manipulate FR systems to mistakenly identify them as pre-defined victims during impersonation attacks. Concurrently, the individuals strive to evade accurate identification as perpetrators, thereby circumventing detection and preventing legal accountability. This requires the creation of adversarial examples capable of executing both impersonation and dodging attacks simultaneously. In the realm of adversarial attacks on image classification, a successful impersonation attack typically implies a successful dodging attack. However, FR is an open-set task [49; 9], which is quite different from image classification. In the real-world deployment of FR systems, accurately predicting the class probability of identities presents an extreme challenge. Therefore, we extract embeddings from two face images using the FR model. Subsequently, the distance between the two embeddings is used to determine whether the images belong to the same identity. If the distance falls below a predefined threshold, the two images are recognized as belonging to the same identity; otherwise, they are classified as different identities. Based on the measurement of FR, there are two decision boundaries for each FR model when crafting adversarial examples as shown in Fig. 1. As a result, there exists the natural samples that can be classified as two different identities in theory. We denote these samples as *multi-identity samples* (refer to Section 4.4).

The existence of multi-identity samples implies that a successful impersonation attack on FR does not necessarily guarantee a successful dodging attack on FR. Existing research indicates that an adversarial sample was located near the decision boundary [18; 4]. Suppose we generate adversarial face examples using previous methods. In the white-box setting, both the structures and parameters of the victim models are known, enabling the generation of adversarial face examples that can cross the decision boundaries of both attacker and victim, as shown in Fig. 1. However, in the black-box setting, the decision boundaries of black-box models differ from those of the surrogate models. Consequently, adversarial examples generated on the surrogate model lie near the decision boundary

of the victim, preventing them from crossing the decision boundary of the attacker. As such, the majority of adversarial face examples crafted by previous methods, which can successfully perform impersonation attacks, fail to perform dodging attacks in the black-box setting.

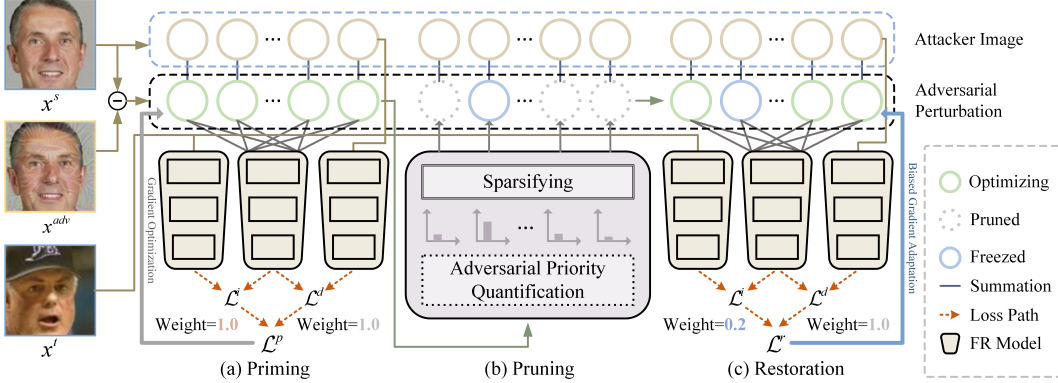


Figure 2: Overview of our Adv-Pruning attack framework, which consists of Priming, Pruning, and Restoration stages. (a) During the Priming stage, we optimize the adversarial examples to ensure they have sufficient attack performance. (b) In the Pruning stage, we propose Adversarial Priority Quantification to quantify the priority of adversarial perturbations. Subsequently, we sparsify the adversarial perturbations based on the quantified priorities. (c) In the Restoration stage, we present Biased Gradient Adaptation to introduce gradient perturbations biased to dodging attacks on the sparsified regions.

In this paper, we propose a novel attack method, termed as Adversarial Pruning (Adv-Pruning). In the realm of adversarial attacks on FR, previous impersonation methods have achieved a significant level of sophistication. However, there remains a pressing need to bolster the efficacy of adversarial face examples in dodging attacks. Consequently, our research is directed towards enhancing the dodging attack performance of adversarial face examples while maintaining the impersonation attack performance. Specifically, we introduce an attack consisting of three stages: Priming, Pruning, and Restoration. In the Priming stage, we optimize the adversarial examples to ensure adequate attack potential. In the Pruning stage, with considering the pruning concept in model compression, we propose Adversarial Priority Quantification to measure the region-wise priority of original adversarial perturbations using an priority measure which is directly proportional to the supremum of the absolute model output variances. After processing by Adversarial Priority Quantification, we prune the adversarial face examples to free up less prioritized adversarial perturbations. In the Restoration stage, we propose Biased Gradient Adaptation to add biased gradient perturbations favoring dodging attacks on the pruned regions to adapt the adversarial face examples into the space that can be classified as the victim while remaining unidentifiable as the attacker, thereby enhancing the dodging performance of the adversarial face examples without compromising the prioritized features of original adversarial perturbations. As illustrated in the top of Fig. 1, after undergoing these stages, the adversarial face example generated by our proposed method can successfully traverse the decision boundaries of both the attacker and victim of the black-box model, achieving successful black-box impersonation and dodging attacks.

Our main contributions are summarized as follows:

- We offer a new perspective for adversarial attacks on FR models that the generation of adversarial examples should perform both impersonation and dodging attacks simultaneously. To the best of our knowledge, this is the first work that studies the universality of multi-identity samples among adversarial face examples crafted by impersonation attacks.
- We propose a novel adversarial attack method called Adversarial Pruning (Adv-Pruning). Adversarial Priority Quantification is presented to quantify the priority of the adversarial perturbations with minimal impact on absolute model output variances. Biased Gradient Adaptation is designed to adapt the adversarial examples to traverse both the decision boundaries of attacker and victim using biased gradients.

- Extensive experiments demonstrate that our proposed method achieves superior performance compared to the state-of-the-art adversarial attack methods. Moreover, our presented method could be plugged into various FR systems and adversarial attack methods.

2 Related Work

2.1 Adversarial Attacks

The primary objective of adversarial attacks is to introduce imperceptible perturbations to benign images to deceive machine learning systems and cause them to make mistakes [47; 14]. The existence of adversarial examples poses a significant threat to the security of current machine learning systems. Lots of efforts have been dedicated to researching adversarial attacks in order to enhance the robustness of these systems [33; 69; 30; 55; 34; 43; 12; 73; 68; 37]. To improve the performance of black-box adversarial attacks, DI [60] applies random transformations to adversarial examples in each iteration to achieve a data augmentation effect. VMI-FGSM [53] employs gradient variance to stabilize the updating process of adversarial examples, boosting the black-box performance. SSA [33] transforms adversarial examples into the frequency domain and uses spectrum transformation to augment them. SIA [54] applies a random image transformation to each image block, generating a varied collection of images that are then employed for gradient calculation. BSR [51] divides the input image into multiple blocks, subsequently shuffling and rotating these blocks in a random manner, creating a collection of new images for the purpose of gradient calculation. DA [16] utilizes dispersion amplification to enhance the multi-task attack capability of adversarial attacks. Despite their gratifying progress, these studies neglect the consideration of pruning adversarial examples through introducing pruning methods into the realm of adversarial attacks. In our research, we propose a novel pruning method capable of identifying and freeing up the adversarial perturbations with minimal impact on absolute model output variances, thereby sparsifying regions for adding adversarial perturbations with the aim of dodging capabilities improvement.

2.2 Adversarial Attacks on Face Recognition

Based on the restriction of the adversarial perturbations, adversarial attacks on FR can be classified into two categories: restricted attacks [32; 61; 10; 74; 35; 31; 5] and unrestricted attacks [3; 6; 65; 8; 44; 46; 48; 56; 57]. Restricted attacks on FR are the attacks that generate adversarial examples in a restricted bound (e.g. L_p bound). To enhance the transferability of adversarial attacks on FR, [70] propose DFANet, which applies dropout on the feature maps of the convolutional layers to achieve ensemble-like effects. In addition, [72] introduces BPFA, which further improves the transferability of adversarial attacks on FR by incorporating beneficial perturbations [58] on the feature maps of the FR models, resulting in hard model augmentation effects. [29] leverages extra information from FR-correlated tasks and uses a multi-task optimization framework to enhance the transferability of crafted adversarial examples. The unrestricted adversarial attacks on FR are the attacks that generate adversarial examples without the restriction of a predefined perturbation bound. They mainly focus on physical attacks [59; 63; 28], attribute editing [40; 23] and generating adversarial examples based on makeup transfer [64; 19; 42]. The existing literature on both restricted and unrestricted adversarial attacks on FR systems has successfully enhanced the performance of these attacks. Nevertheless, it remains under-explored in the correlation between impersonation and dodging attacks. This paper elegantly addresses this by investigating the correlation between impersonation and dodging attacks and introducing a novel attack method that bolsters the dodging capabilities while preserving the impersonation capabilities of previous methods.

3 Methodology

3.1 Problem Formulation

Let $\mathcal{F}^{vct}(x)$ denote the FR model used by the victim to extract the embedding from a face image x . We refer to x^s and x^t as the attacker and victim images, respectively. The objective of the impersonation attacks explored in our research is to manipulate \mathcal{F}^{vct} in order to misclassify x^{adv} as x^t , while ensuring that x^{adv} bears a close visual resemblance to x^s . By contrast, the objective of the dodging attacks proposed in this study is to render $\mathcal{F}^{vct}(x)$ unable to identify x^{adv} as x^s ,

while simultaneously ensuring that x^{adv} bears a visual resemblance to x^s . For the sake of clarity and conciseness, the detailed optimization objectives for both impersonation and dodging attacks are provided *in the appendices*.

Few works explore the correlation between impersonation and dodging attacks on FR. In the following, we delve into the correlation between these two types of attacks and propose a novel method to enhance dodging attacks while maintaining impersonation attacks. An overview of the proposed method is illustrated in Fig. 2. As depicted in Fig. 2, our proposed method is structured into three stages: Priming, Pruning, and Restoration. Through the sequential application of these stages, we are able to generate adversarial examples that exhibit a potent combination of impersonation and dodging attack capabilities.

3.2 Exploring the Impersonation and Dodging Attack on Face Recognition

In most cases, the victim model \mathcal{F}^{vct} is not accessible to the attacker, making it extremely challenging to optimize the objectives for black-box attacks directly. To circumvent this issue, a common approach is to leverage a surrogate model \mathcal{F} accessible to the attacker to generate adversarial examples that can be transferred to the victim model for an effective attack [66; 69; 39; 54; 51; 38; 11; 13; 27; 5].

For impersonation attacks, the loss can be formulated as follows:

$$\mathcal{L}^i = \|\phi(\mathcal{F}(x^{adv})) - \phi(\mathcal{F}(x^t))\|_2^2 \quad (1)$$

where $\phi(x)$ represents the operation that normalizes x . x^{adv} is the adversarial example which is initialized with the same value as x^s . The loss function of dodging attacks can be formulated as:

$$\mathcal{L}^d = -\|\phi(\mathcal{F}(x^{adv})) - \phi(\mathcal{F}(x^s))\|_2^2 \quad (2)$$

As the FR task is an open-set task, it is impractical to predict the classes of users during the practical deployment of the FR model. Therefore, we need to compare the distance between two face images to discern whether they depict the same identity or not. Based on the identification method in FR, multi-identity samples exist theoretically. Our experiments verify the existence of such samples among benign face images. The existence of multi-identity samples raises a question:

Does the success of an impersonation attack imply the success of dodging attacks on FR systems?

To this end, we generate adversarial face examples using the previous impersonation attack and evaluate its dodging Attack Success Rate (ASR). Our experiment confirms that the majority of adversarial examples crafted through previous methods, which are successful in performing impersonation attacks, fail to successfully execute dodging attacks in the black-box setting (see Section 4.4).

Nonetheless, in real-world adversarial attacks, attackers do not want the adversarial face examples to be recognized as themselves, as this may lead to legal consequences. Hence, it is crucial to research attack techniques that can execute both impersonation and dodging attacks simultaneously. Previous methods on FR systems have shown a remarkably high level of impersonation ASR in black-box settings. Therefore, our objective is to enhance the dodging performance while maintaining the impersonation effectiveness of previous attack methods.

To accomplish this objective, a straightforward approach is to generate adversarial face examples using a multi-task attack strategy. In the following, we will take the Lagrangian attack strategy as the example for its simplicity. The Lagrangian attack strategy utilizes the following loss function to craft adversarial examples:

$$\mathcal{L} = \lambda\mathcal{L}^i + \mathcal{L}^d \quad (3)$$

However, due to the conflict between the optimization between \mathcal{L}^i and \mathcal{L}^d , there exists a trade-off between the performance of impersonation and dodging performance, leading to subpar performance (See Section 4.4). Suppose we can mitigate the trade-off, we will achieve a better dodging performance while maintaining the impersonation performance.

3.3 Adversarial Pruning Attack

To accomplish this objective, a straightforward approach is to fine-tune the adversarial face examples generated by the Lagrangian attack with a lower λ value in order to enhance the performance of

dodging attacks. However, this method does not enhance the dodging attack performance without compromising the impersonation attack performance (see *Fine-tuning* in Table 3). We contend that this issue arises because the newly introduced adversarial perturbation that favors dodging attacks ends up disrupting the prioritized features of existing adversarial perturbation. While it may improve the performance of dodging attacks, it inevitably diminishes the performance of impersonation attacks. To address this, we introduce new perturbations favoring dodging attacks in regions where original perturbations are not added. Nevertheless, identifying suitable areas for these new perturbations is challenging due to their scarcity. Therefore, we propose a novel pruning method to release less prioritized adversarial perturbations with minimal impact on the absolute model output variances, thereby creating space to introduce perturbations that facilitate dodging attacks.

Our proposed Adv-Pruning can be combined with various adversarial attacks. In the following, we will introduce our proposed Adv-Pruning based on Lagrangian attack in detail. In the Priming Stage, we utilize Eq. (3) as the Priming loss \mathcal{L}^p to craft the adversarial face examples:

$$x_t^{adv} = \prod_{x^s, \epsilon} \left(x_{t-1}^{adv} - \beta \text{sign} \left(\nabla_{x_{t-1}^{adv}} \mathcal{L}^p \right) \right) \quad (4)$$

where t is the iteration of the optimization process of adversarial examples, and β is the step size when optimizing the adversarial face examples in the Priming stage, and $\prod(x)$ is the projection function that projects x onto the L_p norm bound.

Adversarial Priority Quantification. After completing the Priming Stage, we obtain an adversarial example with varying magnitudes of gradient perturbations across different regions. Following this, we proceed to the Pruning stage to process the crafted adversarial example. In order to prune the adversarial perturbation, our initial step is to assess its priority. To estimate this priority, we propose Adversarial Priority Quantification to quantify the priority of adversarial perturbations. Specifically, Adversarial Priority Quantification utilizes the magnitude of the adversarial perturbation as a measure. A lower magnitude implies a lesser impact on the performance of the adversarial examples generated after sparsification, as the supremum of absolute model output variances is directly proportional to the magnitude of the adversarial perturbations. The proof is *in the appendices*.

Let the adversarial examples be x^{adv} . The formula to calculate the priority can be expressed as:

$$\mathcal{I} = |x^{adv} - x^s| \quad (5)$$

where $\mathcal{I} \in \mathbb{R}^{CHW}$. C, H, and W are the channel number, height, and width of the face images, respectively.

Once the priority values of the adversarial perturbations are quantified, we employ these values to release less prioritized adversarial perturbations. Let κ be the sparsity ratio for pruning the adversarial face examples that measure the ratio of perturbations to be set into zero. Let $s = CHW$ be the number of adversarial perturbation elements. We arrange the elements in a flattened vector of \mathcal{I} in ascending order (from the lowest to the highest):

$$\mathcal{Q} = \text{Sort}(\Psi(\mathcal{I})) \quad (6)$$

where Ψ is the flatten operation.

Let \mathcal{W} be the set of the elements of the adversarial perturbations to be pruned. Given the priority calculation method for pruning, the value of \mathcal{W} can be calculated as follows:

$$\mathcal{W} = \mathcal{Q}[: \kappa s] \quad (7)$$

where the colon denotes the slice operation to obtain the first κs elements. The pruning mask, which has the same shape as \mathcal{I} , can be obtained by utilizing \mathcal{W} :

$$\mathcal{M}_{i,j,k} = \begin{cases} 0, & \text{if } \mathcal{I}_{i,j,k} \in \mathcal{W} \\ 1, & \text{if } \mathcal{I}_{i,j,k} \notin \mathcal{W} \end{cases} \quad (8)$$

By utilizing the mask, we can apply the following formula to prune the adversarial example:

$$\bar{x}^{adv} = x^s + (x^{adv} - x^s) \odot \mathcal{M} \quad (9)$$

where \bar{x}^{adv} is the adversarial face example after pruning.

Biased Gradient Adaptation. During the Restoration stage, we restore the adversarial face examples in the previously pruned region using our proposed Biased Gradient Adaptation. Biased Gradient Adaptation using the following loss function to craft gradient biased to the dodging attacks to adapt the crafted adversarial examples into the space that favors dodging attacks.

$$\mathcal{L}^r = \tilde{\lambda}\mathcal{L}^i + \mathcal{L}^d \quad (10)$$

where $\tilde{\lambda}$ is a weight that is lower than λ that is objective for crafting adversarial face examples that favor dodging attacks. The mask representing the regions for restoring the adversarial examples can be denoted as:

$$\mathcal{A} = 1 - \mathcal{M} \quad (11)$$

Subsequently, we utilize the following formula to restore the pruned adversarial face examples:

$$x_t^{adv} = \prod_{x^s, \epsilon} \left(x_n^{adv} + \mathcal{A} \odot \left(x_{t-1}^{adv} - \gamma \text{sign} \left(\nabla_{x_{t-1}^{adv}} \mathcal{L}^r \right) - \bar{x}^{adv} \right) \right) \quad (12)$$

where γ is the step size when optimizing the adversarial face examples in the Restoration stage, \bar{x}^{adv} is the adversarial example crafted by the Priming Stage, and $\nabla_{x_{t-1}^{adv}} \mathcal{L}^r$ is the biased gradient. The pseudo-code of our proposed method based on the Lagrangian attack is illustrated in the appendices.

4 Experiments

4.1 Experimental Setting

Datasets. We opt to use the LFW [20], CelebA-HQ [24], and FFHQ [25] datasets for our experiments. LFW serves as an unconstrained face dataset for FR. CelebA-HQ and FFHQ consists of high-quality images. The LFW and CelebA-HQ utilized in our experiments are identical to those employed in [72; 71], while FFHQ is the corresponding dataset provided by the Sibling-Attack official page, ensuring the consistency for analysis.

Face Recognition Models. The normal trained FR models employed in our experiments include IR152 [17], FaceNet [41], MobileFace (abbreviated as MF) [9], ArcFace [9], CircleLoss [45], CurricularFace [22], MagFace [36], MV-Softmax [52], and NPCFace [67]. IR152, FaceNet, and MF are identical to those used in [64; 19; 72; 71]. ArcFace, CircleLoss, CurricularFace, MagFace, MV-Softmax, and NPCFace are the official models available in FaceX-ZOO [50]. Additionally, we incorporate adversarial robust FR models in our experiments, denoted as IR152^{adv}, FaceNet^{adv}, and MF^{adv}, which are identical to those used in [72]. For calculating the ASR in impersonation and dodging attacks, we choose the thresholds based on FAR@0.001 on the entire LFW dataset.

Attack Setting. Without any particular emphasis, we set the maximum allowable perturbation magnitude to 10 based on the L_∞ norm bound and utilize the Lagrangian attack method as the attack in both the Priming and Restoration stages. Additionally, we specify the maximum number

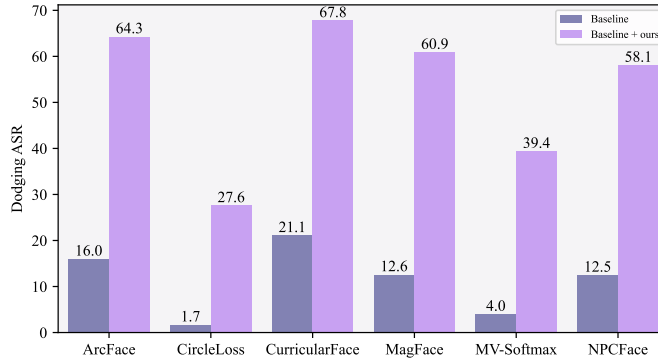


Figure 3: The ASR on FR models trained by multiple algorithms.

Table 1: Comparisons of dodging ASR (%) results for attacks on the LFW and CelebA-HQ datasets. The surrogate models are presented in the first column, and the victim models are listed in the second row. The numbers before and after the slash represent the results of the baseline attack and the attack that combines the baseline attack with our proposed attack, respectively.

Surrogate Model	Attack	LFW			CelebA-HQ		
		IR152	FaceNet	MF	IR152	FaceNet	MF
IR152 [17]	DI	95.4 / 100.0	5.8 / 11.3	0.2 / 0.8	87.9 / 100.0	8.4 / 16.4	0.4 / 1.2
	VMI	92.7 / 100.0	17.3 / 32.5	1.2 / 9.5	92.2 / 100.0	14.3 / 27.9	1.2 / 4.1
	SSA	78.8 / 100.0	5.7 / 22.5	0.9 / 10.6	83.8 / 99.9	7.2 / 19.6	0.4 / 5.6
	DFANet	98.9 / 100.0	1.4 / 4.2	0.0 / 0.3	98.9 / 100.0	2.3 / 6.0	0.0 / 0.4
	SIA	81.7 / 100.0	13.0 / 37.5	0.8 / 8.9	78.4 / 100.0	13.2 / 35.6	0.7 / 7.4
	BSR	52.4 / 100.0	5.3 / 17.6	0.1 / 1.5	48.5 / 99.9	5.4 / 18.0	0.3 / 1.9
	BPFA	92.6 / 100.0	1.7 / 7.3	0.0 / 1.2	90.4 / 100.0	2.1 / 8.1	0.1 / 0.8
FaceNet [41]	DI	5.3 / 10.3	99.8 / 99.9	3.1 / 10.3	1.5 / 3.1	99.4 / 99.9	1.8 / 4.7
	VMI	9.7 / 14.3	99.8 / 99.9	6.2 / 13.2	3.1 / 7.1	99.3 / 99.8	3.6 / 9.3
	SSA	6.0 / 14.0	97.5 / 99.9	6.6 / 26.2	2.0 / 5.5	96.9 / 99.7	4.2 / 14.6
	DFANet	1.6 / 3.3	99.8 / 99.9	0.4 / 2.7	0.5 / 2.6	99.1 / 100.0	0.8 / 4.1
	SIA	11.2 / 20.6	99.5 / 99.9	8.7 / 21.2	4.0 / 8.9	99.4 / 99.9	5.4 / 13.7
	BSR	12.2 / 19.2	98.6 / 99.9	9.0 / 17.8	4.6 / 10.1	98.8 / 99.9	5.3 / 14.1
	BPFA	4.7 / 16.8	98.6 / 100.0	1.6 / 15.0	1.1 / 4.2	99.0 / 100.0	0.6 / 5.1
MF [9]	DI	2.2 / 7.3	18.2 / 36.4	99.2 / 100.0	0.1 / 2.5	12.1 / 31.3	95.2 / 100.0
	VMI	1.0 / 2.8	8.4 / 20.9	99.7 / 100.0	0.2 / 0.4	5.2 / 15.0	98.2 / 100.0
	SSA	0.7 / 4.1	6.1 / 23.5	98.3 / 100.0	0.0 / 0.6	3.9 / 18.5	93.3 / 100.0
	DFANet	0.2 / 1.0	1.5 / 5.8	99.6 / 100.0	0.0 / 0.2	1.1 / 7.7	99.1 / 100.0
	SIA	1.0 / 5.9	10.6 / 36.6	98.4 / 100.0	0.1 / 2.4	9.0 / 24.4	96.3 / 100.0
	BSR	0.4 / 1.5	3.7 / 14.7	84.9 / 100.0	0.1 / 0.6	2.9 / 12.6	77.6 / 100.0
	BPFA	0.9 / 4.1	4.6 / 20.4	97.7 / 100.0	0.0 / 2.3	4.0 / 20.4	96.2 / 100.0

of iterative steps as 200. For both the Priming and Restoration stages, the step size is uniformly designated as 1.0.

Evaluation Metrics. We employ Attack Success Rate (ASR) to evaluate the performance of various attacks. ASR signifies the proportion of successfully attacked adversarial examples out of all the adversarial examples. We use ASR^i and ASR^d to denote impersonation and dodging ASR, respectively. The detailed calculation methods for ASR^i and ASR^d are provided in the appendices.

Compared methods. Our proposed attack is a restricted attack method that aims to maliciously attack FR systems to expose more blind spots of them. It is not fair to compare our proposed method with unrestricted attacks that do not limit the magnitude of the adversarial perturbations. Therefore, we choose restricted attacks on FR that aim to maliciously attack FR systems [70] [72] [29] and state-of-the-art transfer attacks [60] [33] [54] [51] as our baseline.

4.2 Comparison Study

We compare our proposed attack method with the state-of-the-art attacks on multiple FR models and datasets. Several adversarial examples are illustrated in Fig. 5. The attack performance results are shown in Table 1. Table 1 illustrates that the incorporation of our proposed attack method

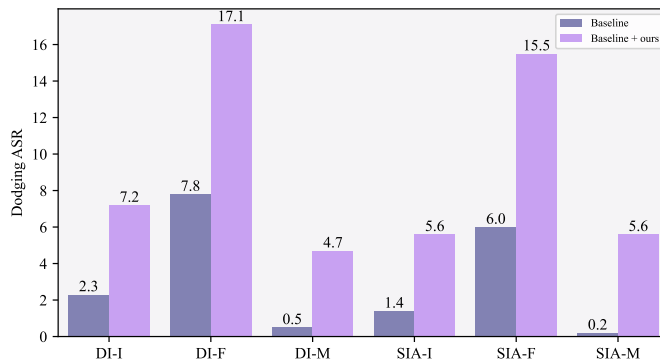


Figure 4: Comparisons of ASR (%) on LFW with adversarial robust models as victim models.

Table 2: Comparisons of ASR (%) with multi-task attacks on LFW dataset. Models in the second row are victim models.

Attack	IR152	ASR ^d		ASR ⁱ
		FaceNet	MF	
Lagrangian	3.9	26.5	100.0	26.0
Lagrangian + ours	7.3	36.4	100.0	26.6
DA	11.0	35.6	99.1	37.4
DA + ours	17.5	44.9	99.4	37.8

significantly enhances the dodging ASR of adversarial attacks. It is worth noting that the average black-box impersonation ASRs of the baseline attacks in Table 1 also increase after integrating our proposed attack method. This demonstrates the effectiveness of our proposed method in improving the dodging attack performance while simultaneously maintaining the impersonation attack performance. Furthermore, we conducted a comparison between our proposed Adv-Pruning and multi-task attacks using MF as the surrogate model on LFW based on DI. For our proposed method, we choose the corresponding multi-task attack as the attack for both the Priming and Restoration stages. The dodging ASR and average black-box impersonation ASR results are shown in Table 2. Table 2 underscores the effectiveness of our method in enhancing the dodging performance of multi-task attacks while maintaining the impersonation performance. To further validate our proposed attack method on additional FR models, we selected SIA [54] as Baseline and IR152 as the surrogate model. The experimental settings are consistent with those described in Table 1. The dodging ASR across multiple FR models is demonstrated in Fig. 3. As depicted in Fig. 3, the dodging ASR improves on multiple FR models after integrating our proposed method, further confirming the effectiveness of our attack.

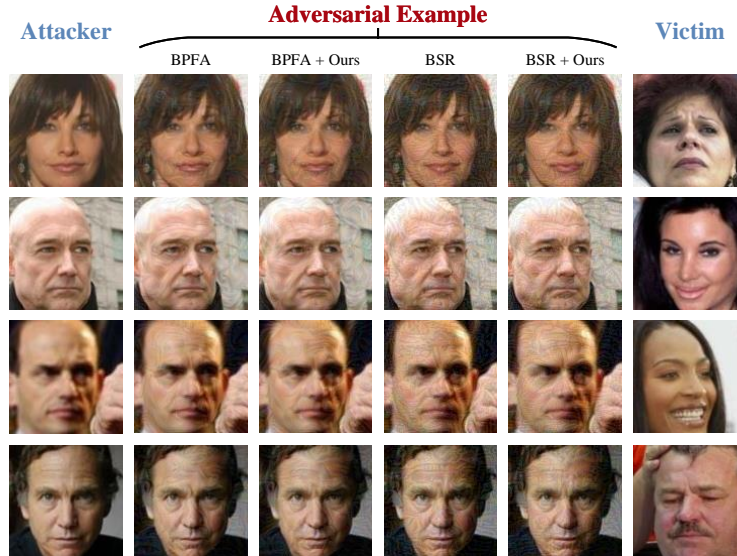


Figure 5: The Illustration of adversarial examples crafted by various attacks. First column: some attacker images. Last column: the corresponding victim images. The second to fifth columns exhibit the corresponding adversarial face examples crafted by BPFA, BPFA + ours, BSR, and BSR + ours, respectively.

In practical application scenarios, victims can employ adversarial robust models to defend against adversarial attacks. Consequently, it becomes crucial to evaluate the performance of adversarial attacks on these robust models. In this study, we generate adversarial examples on the LFW dataset using MF as the surrogate model and assess the performance of various attacks on the adversarial robust models. The results are presented in Fig. 4. The letters following the en dash represent the surrogate models, with 'I', 'F', and 'M' corresponding to $IR152^{adv}$, $FaceNet^{adv}$, and MF^{adv} , respectively. Fig. 4 illustrates that the inclusion of our proposed method leads to improvements in

both dodging and impersonation performance. These results serve as evidence of the effectiveness of our proposed method on adversarial robust models.

JPEG compression is a widely adopted method for image compression during transmission, concurrently acting as a defense mechanism against adversarial examples. To assess the effectiveness of our proposed attack under JPEG compression, we utilize DI as the baseline attack and MF as the surrogate model, evaluating the attack performance on ArcFace and CurricularFace models with experimental settings consistent with those described in Table 1. The results are illustrated in Fig. 6. These results demonstrate that across varying levels of JPEG compression, our proposed attack method consistently outperforms the baseline attack, thereby highlighting its effectiveness under JPEG compression.

The experimental results on negative cosine similarity loss, and Sibling-Attack are presented *in the appendices*.

4.3 Ablation Study

To delve into the properties of our proposed attack method, we conducted an ablation experiment using DI as the Baseline attack, with MF serving as the surrogate model on the LFW dataset. To confirm the effectiveness of our pruning method, we employed the Random Zeroing (RZ) method, which randomly sets adversarial perturbations to zero. We applied this method and our pruning method to free up 20% of the adversarial perturbations crafted by the Lagrangian attack. For *Fine-tuning*, we employed the Lagrangian attack as the method to further optimize the Lagrangian adversarial examples with a lower λ . The dodging attack ASR and average black-box impersonation ASR results are shown in Table 3. Table 3 demonstrates that our proposed pruning method for adversarial examples achieves a significantly smaller decrease in ASR than RZ after pruning 20% of adversarial perturbations, indicating the effectiveness of our pruning method. After being processed using the Pruning and Restoration stage of our proposed Adv-Pruning method, both impersonation and dodging ASR of the crafted adversarial face examples are recovered and higher than the Baseline attack method. These results demonstrate the effectiveness of our proposed Adv-Pruning in improving the dodging performance of adversarial attacks on FR without compromising the impersonation attack performance.

The sparsity ratio quantifies the proportion of adversarial perturbations that are allowed to be discarded during the Pruning stage. This ratio greatly impacts the performance of our proposed attack method. Hence, we conducted a sensitivity study on the sparsity ratio to analyze its effect on performance of the algorithm. The Lagrangian attack method based on DI is selected as the Baseline. We conduct a hyperparameter sensitivity study on LFW using FaceNet as the surrogate model, and adjust the value of $\tilde{\lambda}$ to ensure that the average black-box impersonation ASR results were within a 0.4% absolute difference compared to the Baseline. The dodging ASR results are illustrated in the right plot of Fig. 7. The results illustrate that the dodging ASR of our proposed method initially increases and then decreases as the sparsity ratio increases. When the sparsity ratio increases, a greater number of adversarial perturbations are pruned, creating more empty regions for the adversarial perturbations that favor dodging attacks in the Restoration stage. If the sparsity ratio is set to a too-high value, an excessive number of adversarial perturbations are allowed to be freed up, resulting in a degradation of performance for the adversarial examples crafted by the Priming stage. Consequently, the performance of adversarial face examples will decrease.

4.4 Analytical Study

Multi-identity Samples among the Natural Face Images: Multi-identity samples are intriguing samples that can be classified as multiple classes in FR. In this section, we will explore the existence of multi-identity samples among the natural face images. We randomly select negative face pairs from the entire LFW dataset. Subsequently, we use MF as our FR model to extract the embeddings of the face images in each face pair and calculate the cosine similarity between the two images. If the cosine similarity surpasses the threshold, both images in the pair are classified as belonging to multiple identities, indicating that they are multi-identity samples. Our findings demonstrate the presence of multi-identity samples among the benign face images, as illustrated in the bottom left of Fig. 1. The multi-identity samples in Fig. 1 closely resemble the appearances of the identities they are classified into.

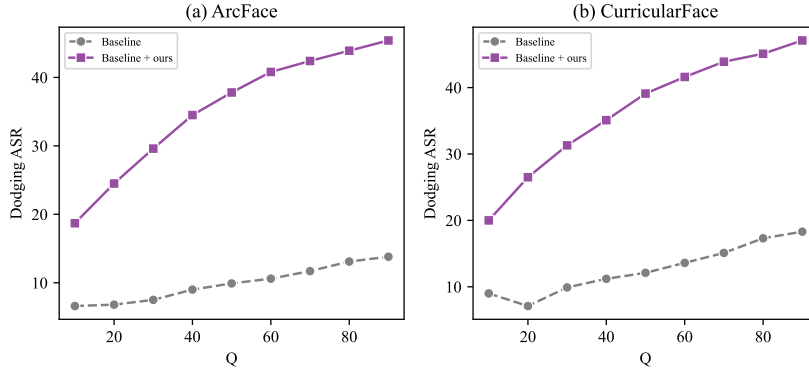


Figure 6: The dodging ASR under various JPEG Q values.

Table 3: Comparisons of ASR (%) results of dodging attack and impersonation attacks on the LFW dataset. The models in the second row are the victim models.

Attack	ASR ^d			ASR ⁱ
	IR152	FaceNet	MF	
Baseline	2.2	18.2	99.2	25.6
Lagrangian	3.9	26.5	100.0	26.0
<i>Fine-tuning</i>	4.2	26.3	100.0	25.6
<i>RZ</i>	0.6	4.4	94.8	15.1
<i>Pruning</i>	3.4	24.8	100.0	25.4
Adv-Pruning	5.4	32.5	100.0	26.3

To analyze the cause of this phenomenon, we need to consider the properties of both the multi-identity samples and the FR model. Commonly-used FR models are well-trained and capable of correctly classifying the majority of benign face images. However, there are some benign face images that the FR model fails to classify accurately, and these samples are referred to as hard samples [21; 72]. Multi-identity samples are a specific type of hard sample known as hard negative samples. Typically, hard negative samples exhibit a similar appearance [67], indicating that the multi-identity samples among the benign face images share a resemblance.

Universality of Multi-identity Samples among Adversarial Face Examples: The previous impersonation methods craft adversarial face examples only use the impersonation loss \mathcal{L}^i . In this section, we will investigate the ratio of multi-identity samples and evaluate the effectiveness of previous impersonation methods in terms of dodging attacks. We utilize the Multi-identity Sample Ratio (MSR) to gauge the proportion of multi-identity samples in the adversarial face examples capable of executing successful impersonation attacks. These multi-identity samples can be recognized as both the attacker and victim identities in the setting of our paper. The detailed calculation method of MSR is *in the appendices*. We evaluate the MSR, impersonation ASR and dodging ASR using MF as the surrogate model on the LFW dataset and the results are demonstrated *in the appendices*. The results demonstrates that most of the crafted adversarial face examples are multi-identity samples in the black-box setting. This indicates that most adversarial face examples generated through previous impersonation attacks are unable to attain a successful dodging attack in the black-box setting. Nevertheless, in the white-box setting, the majority of adversarial face examples capable of executing successful impersonation attacks also demonstrate success in dodging attacks.

To analyze the reason, we consider the metric used to determine whether two face images belong to the same identity in FR. Since FR is an open-set task, we rely on the distance in the embedding space to make decisions. The top of Fig. 1 illustrates two decision boundaries for each FR model, one for attacker identity and one for victim identity. In the white-box setting, if we generate adversarial examples using \mathcal{L}^i , these adversarial examples can penetrate a space where they are recognized as the victim identity rather than the attacker identity. However, the decision boundary of the black-box

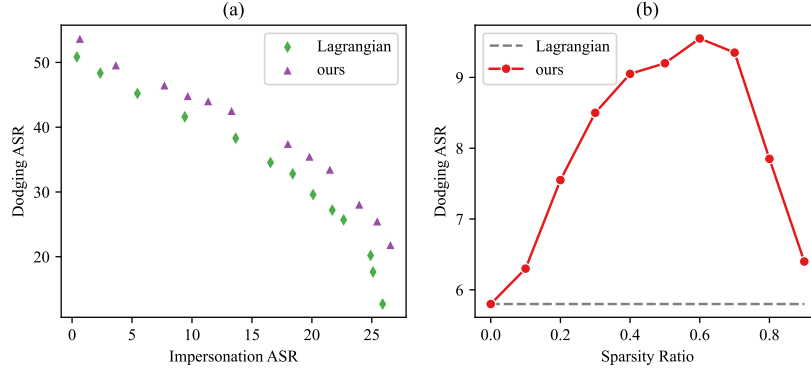


Figure 7: (a) The trade-off between the ASR (%) of impersonation attack and dodging attack of adversarial examples. (b) The dodging ASR (%) in different sparsity ratios.

model differs from that of the surrogate model. In the black-box setting, most adversarial examples are found between the decision boundaries of the black-box model, resulting in the majority of adversarial examples crafted using \mathcal{L}^i being multi-identity samples. This demonstrates that the adversarial face examples are positioned near the decision boundary in the black-box setting.

The Trade-off Between the Impersonation Attacks and Dodging Attacks: Owing to the inherent conflict during the optimization process of impersonation and dodging losses in the black-box setting, there exists a trade-off between impersonation and dodging performance. We craft adversarial face examples using Lagrangian attack and our proposed Adv-Pruning on LFW based on DI. The average black-box results are demonstrated in the left plot of Fig. 7.

The results illustrate that our proposed method can reduce the trade-off between impersonation and dodging performance in the black-box setting. The pruning operation of our proposed Adv-Pruning serves to sparsify the adversarial perturbations while preserving the impersonation performance. On the other hand, the restoration operation tends to introduce adversarial perturbations in the pruned areas, specifically favoring dodging attacks. These operations effectively enhance the dodging attack performance while maintaining the impersonation attack performance, ultimately mitigating the trade-off.

5 Conclusion

In this paper, we reveal the universality of multi-identity samples among adversarial face examples crafted by previous impersonation attacks and the success of an impersonation attack may not necessarily imply the success of dodging attacks on FR systems in the black-box setting. In order to improve dodging performance without compromising impersonation performance, we proposed a novel attack, namely Adv-Pruning. Adv-Pruning comprises Priming, Pruning, and Restoration Stages. Leveraging our proposed Adversarial Priority Quantification, we identify less prioritized adversarial perturbations with minimal impact on absolute model output variances. Through our proposed Biased Gradient Adaptation, biased gradient perturbations are applied to the sparsified regions, adapting adversarial face examples to a space favoring dodging attacks. Extensive experiments demonstrate the effectiveness of our proposed method.

References

- [1] Xiang An, Xuhan Zhu, Yuan Gao, Yang Xiao, Yongle Zhao, Ziyong Feng, Lan Wu, Bin Qin, Ming Zhang, Debing Zhang, and Ying Fu. Partial FC: training 10 million identities on a single machine. In *IEEE/CVF International Conference on Computer Vision Workshops*, pages 1445–1449. IEEE, 2021.

- [2] Fadi Boutros, Jonas Henry Grebe, Arjan Kuijper, and Naser Damer. Idiff-face: Synthetic-based face recognition through fizzy identity-conditioned diffusion models. In *IEEE/CVF International Conference on Computer Vision*, pages 19593–19604. IEEE, 2023.
- [3] Tom B. Brown, Nicholas Carlini, Chiyuan Zhang, Catherine Olsson, Paul F. Christiano, and Ian J. Goodfellow. Unrestricted adversarial examples. *CoRR*, abs/1809.08352, 2018.
- [4] Xiaoyu Cao and Neil Zhenqiang Gong. Mitigating evasion attacks to deep neural networks via region-based classification. *Proceedings of the 33rd Annual Computer Security Applications Conference*, 2017.
- [5] Bin Chen, Jia-Li Yin, Shukai Chen, Bohao Chen, and Ximeng Liu. An adaptive model ensemble adversarial attack for boosting adversarial transferability. In *International Conference on Computer Vision*, pages 4466–4475. IEEE, 2023.
- [6] Zhaoyu Chen, Bo Li, Shuang Wu, Kaixun Jiang, Shouhong Ding, and Wenqiang Zhang. Content-based unrestricted adversarial attack. In *Advances in Neural Information Processing Systems*, 2023.
- [7] Valeriia Cherepanova, Micah Goldblum, Harrison Foley, Shiyuan Duan, John P Dickerson, Gavin Taylor, and Tom Goldstein. Lowkey: Leveraging adversarial attacks to protect social media users from facial recognition. In *International Conference on Learning Representations*, 2021.
- [8] Xuelong Dai, Kaisheng Liang, and Bin Xiao. Advdiff: Generating unrestricted adversarial examples using diffusion models. *CoRR*, abs/2307.12499, 2023.
- [9] Jiankang Deng, Jia Guo, Jing Yang, Niannan Xue, Irene Kotsia, and Stefanos Zafeiriou. Arcface: Additive angular margin loss for deep face recognition. *IEEE Transactions on Pattern Analysis and Machine Intelligence*, 44(10):5962–5979, 2022.
- [10] Yinpeng Dong, Fangzhou Liao, Tianyu Pang, Hang Su, Jun Zhu, Xiaolin Hu, and Jianguo Li. Boosting adversarial attacks with momentum. *Proceedings of the IEEE Conference on Computer Vision and Pattern Recognition*, pages 9185–9193, 2018.
- [11] Junqi Gao, Biqing Qi, Yao Li, Zhichang Guo, Dong Li, Yuming Xing, and Dazhi Zhang. Perturbation towards easy samples improves targeted adversarial transferability. In *Advances in Neural Information Processing Systems*, 2023.
- [12] Zhijin Ge, Fanhua Shang, Hongying Liu, Yuanyuan Liu, Liang Wan, Wei Feng, and Xiaosen Wang. Improving the transferability of adversarial examples with arbitrary style transfer. In *Proceedings of the 31st ACM International Conference on Multimedia*, pages 4440–4449, 2023.
- [13] Zhijin Ge, Xiaosen Wang, Hongying Liu, Fanhua Shang, and Yuanyuan Liu. Boosting adversarial transferability by achieving flat local maxima. In *Advances in Neural Information Processing Systems*, 2023.
- [14] Ian J Goodfellow, Jonathon Shlens, and Christian Szegedy. Explaining and harnessing adversarial examples. In *International Conference on Learning Representations*, 2015.
- [15] Yiwen Guo, Qizhang Li, and Hao Chen. Backpropagating linearly improves transferability of adversarial examples. *Advances in neural information processing systems*, 33:85–95, 2020.
- [16] Pavlo Haleta, Dmytro Likhomanov, and Oleksandra Sokol. Multitask adversarial attack with dispersion amplification. *EURASIP Journal on Information Security*, 2021:1–10, 2021.
- [17] Kaiming He, Xiangyu Zhang, Shaoqing Ren, and Jian Sun. Deep residual learning for image recognition. In *2016 IEEE Conference on Computer Vision and Pattern Recognition, CVPR 2016, Las Vegas, NV, USA, June 27-30, 2016*, pages 770–778. IEEE Computer Society, 2016.
- [18] Byeongho Heo, Minsik Lee, Sangdoo Yun, and Jin Young Choi. Knowledge distillation with adversarial samples supporting decision boundary. In *The Thirty-Third AAAI Conference on Artificial Intelligence*, pages 3771–3778. AAAI Press, 2019.

- [19] Shengshan Hu, Xiaogeng Liu, Yechao Zhang, Minghui Li, Leo Yu Zhang, Hai Jin, and Libing Wu. Protecting facial privacy: Generating adversarial identity masks via style-robust makeup transfer. In *Proceedings of the IEEE conference on computer vision and pattern recognition*, pages 14994–15003, 2022.
- [20] Gary B. Huang, Manu Ramesh, Tamara Berg, and Erik Learned-Miller. Labeled faces in the wild: A database for studying face recognition in unconstrained environments. Technical Report 07-49, University of Massachusetts, Amherst, October 2007.
- [21] Y. Huang, Pengcheng Shen, Ying Tai, Shaoxin Li, Xiaoming Liu, Jilin Li, Feiyue Huang, and Rongrong Ji. Improving face recognition from hard samples via distribution distillation loss. In *European Conference on Computer Vision*, 2020.
- [22] Yuge Huang, Yuhan Wang, Ying Tai, Xiaoming Liu, Pengcheng Shen, Shaoxin Li, Jilin Li, and Feiyue Huang. Curricularface: Adaptive curriculum learning loss for deep face recognition. In *IEEE/CVF Conference on Computer Vision and Pattern Recognition*, 2020.
- [23] Shuai Jia, Bangjie Yin, Taiping Yao, Shouhong Ding, Chunhua Shen, Xiaokang Yang, and Chao Ma. Adv-attribute: Inconspicuous and transferable adversarial attack on face recognition. In *NeurIPS*, 2022.
- [24] Tero Karras, Timo Aila, Samuli Laine, and Jaakko Lehtinen. Progressive growing of gans for improved quality, stability, and variation. In *International Conference on Learning Representation*, 2018.
- [25] Tero Karras, Samuli Laine, and Timo Aila. A style-based generator architecture for generative adversarial networks. In *2019 IEEE/CVF Conference on Computer Vision and Pattern Recognition (CVPR)*, pages 4396–4405, 2019.
- [26] Jingzhi Li, Zidong Guo, Hui Li, Seungju Han, Ji-Won Baek, Min Yang, Ran Yang, and Sungjoo Suh. Rethinking feature-based knowledge distillation for face recognition. In *IEEE/CVF Conference on Computer Vision and Pattern Recognition*, pages 20156–20165. IEEE, 2023.
- [27] Qizhang Li, Yiwen Guo, Wangmeng Zuo, and Hao Chen. Improving adversarial transferability via intermediate-level perturbation decay. In *Advances in Neural Information Processing Systems*, 2023.
- [28] Yanjie Li, Yiquan Li, Xuelong Dai, Songtao Guo, and Bin Xiao. Physical-world optical adversarial attacks on 3d face recognition. In *2023 IEEE/CVF Conference on Computer Vision and Pattern Recognition (CVPR)*, pages 24699–24708, 2023.
- [29] Zexin Li, Bangjie Yin, Taiping Yao, Junfeng Guo, Shouhong Ding, Simin Chen, and Cong Liu. Sibling-attack: Rethinking transferable adversarial attacks against face recognition. In *IEEE/CVF Conference on Computer Vision and Pattern Recognition, CVPR 2023, Vancouver, BC, Canada, June 17-24, 2023*, pages 24626–24637. IEEE, 2023.
- [30] Chumeng Liang, Xiaoyu Wu, Yang Hua, Jiaru Zhang, Yiming Xue, Tao Song, Zhengui Xue, Ruhui Ma, and Haibing Guan. Adversarial example does good: Preventing painting imitation from diffusion models via adversarial examples. In *International Conference on Machine Learning*, pages 20763–20786. PMLR, 2023.
- [31] Xuannan Liu, Yaoyao Zhong, Yuhang Zhang, Lixiong Qin, and Weihong Deng. Enhancing generalization of universal adversarial perturbation through gradient aggregation. In *IEEE/CVF International Conference on Computer Vision*, pages 4412–4421. IEEE, 2023.
- [32] Yiran Liu, Xin Feng, Yunlong Wang, Wu Yang, and Di Ming. TRM-UAP: enhancing the transferability of data-free universal adversarial perturbation via truncated ratio maximization. In *IEEE/CVF International Conference on Computer Vision*, pages 4739–4748. IEEE, 2023.
- [33] Yuyang Long, Qilong Zhang, Boheng Zeng, Lianli Gao, Xianglong Liu, Jian Zhang, and Jingkuan Song. Frequency domain model augmentation for adversarial attack. In *European conference on computer vision*, volume 13664, pages 549–566, 2022.

- [34] Dong Lu, Zhiqiang Wang, Teng Wang, Weili Guan, Hongchang Gao, and Feng Zheng. Set-level guidance attack: Boosting adversarial transferability of vision-language pre-training models. In *Proceedings of the IEEE/CVF International Conference on Computer Vision*, pages 102–111, 2023.
- [35] Dong Lu, Zhiqiang Wang, Teng Wang, Weili Guan, Hongchang Gao, and Feng Zheng. Set-level guidance attack: Boosting adversarial transferability of vision-language pre-training models. In *IEEE/CVF International Conference on Computer Vision*, pages 102–111. IEEE, 2023.
- [36] Qiang Meng, Shichao Zhao, Zhida Huang, and Feng Zhou. Magface: A universal representation for face recognition and quality assessment. In *IEEE Conference on Computer Vision and Pattern Recognition*, pages 14225–14234. Computer Vision Foundation / IEEE, 2021.
- [37] Duan Mingxing, Kenli Li, Lingxi Xie, Qi Tian, and Bin Xiao. Towards multiple black-boxes attack via adversarial example generation network. In *Proceedings of the 29th ACM International Conference on Multimedia*, pages 264–272, 2021.
- [38] Krishna kanth Nakka and Mathieu Salzmann. Learning transferable adversarial perturbations. In *Advances in Neural Information Processing Systems*, volume 34, pages 13950–13962. Curran Associates, Inc., 2021.
- [39] Muzammal Naseer, Ahmad Mahmood, Salman Khan, and Fahad Khan. Boosting adversarial transferability using dynamic cues. In *International Conference on Learning Representations*, 2023.
- [40] Haonan Qiu, Chaowei Xiao, Lei Yang, Xinchun Yan, Honglak Lee, and Bo Li. Semanticadv: Generating adversarial examples via attribute-conditioned image editing. In *Computer Vision—ECCV 2020: 16th European Conference, Glasgow, UK, August 23–28, 2020, Proceedings, Part XIV 16*, pages 19–37. Springer, 2020.
- [41] Florian Schroff, Dmitry Kalenichenko, and James Philbin. Facenet: A unified embedding for face recognition and clustering. In *Proceedings of the IEEE Conference on Computer Vision and Pattern Recognition*, pages 815–823, 2015.
- [42] Fahad Shamsad, Muzammal Naseer, and Karthik Nandakumar. Clip2protect: Protecting facial privacy using text-guided makeup via adversarial latent search. In *Proceedings of the IEEE/CVF Conference on Computer Vision and Pattern Recognition*, pages 20595–20605, 2023.
- [43] Erfan Shayegani, Yue Dong, and Nael Abu-Ghazaleh. Jailbreak in pieces: Compositional adversarial attacks on multi-modal language models. In *The Twelfth International Conference on Learning Representations*, 2024.
- [44] Florian Stimberg, Ayan Chakrabarti, Chun-Ta Lu, Hussein Hazimeh, Otilia Stretcu, Wei Qiao, Yintao Liu, Merve Kaya, Cyrus Rashtchian, Ariel Fuxman, Mehmet Tek, and Sven Gowal. Benchmarking robustness to adversarial image obfuscations. In *Advances in Neural Information Processing Systems*, 2023.
- [45] Yifan Sun, Changmao Cheng, Yuhan Zhang, Chi Zhang, Liang Zheng, Zhongdao Wang, and Yichen Wei. Circle loss: A unified perspective of pair similarity optimization. In *IEEE/CVF Conference on Computer Vision and Pattern Recognition*, 2020.
- [46] Naufal Suryanto, Yongsu Kim, Harashta Tatimma Larasati, Hyoeun Kang, Thi-Thu-Huong Le, Yoonyoung Hong, Hunmin Yang, Se-Yoon Oh, and Howon Kim. ACTIVE: towards highly transferable 3d physical camouflage for universal and robust vehicle evasion. In *IEEE/CVF International Conference on Computer Vision*, pages 4282–4291. IEEE, 2023.
- [47] Christian Szegedy, Wojciech Zaremba, Ilya Sutskever, Joan Bruna, Dumitru Erhan, Ian J. Goodfellow, and Rob Fergus. Intriguing properties of neural networks. In Yoshua Bengio and Yann LeCun, editors, *2nd International Conference on Learning Representations, ICLR 2014, Banff, AB, Canada, April 14-16, 2014, Conference Track Proceedings*, 2014.
- [48] Donghua Wang, Wen Yao, Tingsong Jiang, Chao Li, and Xiaoqian Chen. RFLA: A stealthy reflected light adversarial attack in the physical world. In *IEEE/CVF International Conference on Computer Vision*, pages 4432–4442. IEEE, 2023.

- [49] Hao Wang, Yitong Wang, Zheng Zhou, Xing Ji, Dihong Gong, Jingchao Zhou, Zhifeng Li, and Wei Liu. Cosface: Large margin cosine loss for deep face recognition. In *IEEE/CVF Conference on Computer Vision and Pattern Recognition*, 2018.
- [50] Jun Wang, Yinglu Liu, Yibo Hu, Hailin Shi, and Tao Mei. Facex-zoo: A pytorch toolbox for face recognition. 2021.
- [51] Kunyu Wang, Xuanran He, Wenxuan Wang, and Xiaosen Wang. Boosting adversarial transferability by block shuffle and rotation. *arXiv preprint arXiv:2308.10299*, 2023.
- [52] Xiaobo Wang, Shifeng Zhang, Shuo Wang, Tianyu Fu, Hailin Shi, and Tao Mei. Mis-classified vector guided softmax loss for face recognition. In *The Thirty-Fourth AAAI Conference on Artificial Intelligence*, pages 12241–12248. AAAI Press, 2020.
- [53] Xiaosen Wang and Kun He. Enhancing the transferability of adversarial attacks through variance tuning. In *Proceedings of the IEEE Conference on Computer Vision and Pattern Recognition*, pages 1924–1933, 2021.
- [54] Xiaosen Wang, Zeliang Zhang, and Jianping Zhang. Structure invariant transformation for better adversarial transferability. In *Proceedings of the IEEE/CVF International Conference on Computer Vision*, pages 4607–4619, 2023.
- [55] Xingxing Wei, Yao Huang, Yitong Sun, and Jie Yu. Unified adversarial patch for cross-modal attacks in the physical world. In *Proceedings of the IEEE/CVF International Conference on Computer Vision*, pages 4445–4454, 2023.
- [56] Xingxing Wei, Yao Huang, Yitong Sun, and Jie Yu. Unified adversarial patch for cross-modal attacks in the physical world. In *IEEE/CVF International Conference on Computer Vision*, pages 4422–4431. IEEE, 2023.
- [57] Xingxing Wei, Jie Yu, and Yao Huang. Physically adversarial infrared patches with learnable shapes and locations. In *IEEE/CVF Conference on Computer Vision and Pattern Recognition*, pages 12334–12342. IEEE, 2023.
- [58] Shixian Wen and Laurent Itti. Beneficial perturbations network for defending adversarial examples. *arXiv preprint arXiv:2009.12724*, 2020.
- [59] Zihao Xiao, Xianfeng Gao, Chilin Fu, Yinpeng Dong, Wei Gao, Xiaolu Zhang, Jun Zhou, and Jun Zhu. Improving transferability of adversarial patches on face recognition with generative models. In *Proceedings of the IEEE conference on computer vision and pattern recognition*, pages 11840–11849, 2021.
- [60] Cihang Xie, Zhishuai Zhang, Yuyin Zhou, Song Bai, Jianyu Wang, Zhou Ren, and Alan L. Yuille. Improving transferability of adversarial examples with input diversity. In *Proceedings of the IEEE Conference on Computer Vision and Pattern Recognition*, pages 2730–2739, 2019.
- [61] Zhuoer Xu, Zhangxuan Gu, Jianping Zhang, Shiwen Cui, Changhua Meng, and Weiqiang Wang. Backpropagation path search on adversarial transferability. In *IEEE/CVF International Conference on Computer Vision*, pages 4640–4650. IEEE, 2023.
- [62] Xiao Yang, Yinpeng Dong, Tianyu Pang, Hang Su, Jun Zhu, Yuefeng Chen, and Hui Xue. Towards face encryption by generating adversarial identity masks. In *Proceedings of the IEEE International Conference on Computer Vision*, pages 3877–3887, 2021.
- [63] Xiao Yang, Chang Liu, Longlong Xu, Yikai Wang, Yinpeng Dong, Ning Chen, Hang Su, and Jun Zhu. Towards effective adversarial textured 3d meshes on physical face recognition. In *2023 IEEE/CVF Conference on Computer Vision and Pattern Recognition (CVPR)*, pages 4119–4128, 2023.
- [64] Bangjie Yin, Wenxuan Wang, Taiping Yao, Junfeng Guo, Zelun Kong, Shouhong Ding, Jilin Li, and Cong Liu. Adv-makeup: A new imperceptible and transferable attack on face recognition. In *International Joint Conference on Artificial Intelligence*, pages 1252–1258, 2021.

- [65] Shengming Yuan, Qilong Zhang, Lianli Gao, Yaya Cheng, and Jingkuan Song. Natural color fool: Towards boosting black-box unrestricted attacks. In *Advances in Neural Information Processing Systems*, 2022.
- [66] Zheng Yuan, Jie Zhang, and Shiguang Shan. Adaptive image transformations for transfer-based adversarial attack. In Shai Avidan, Gabriel J. Brostow, Moustapha Cissé, Giovanni Maria Farinella, and Tal Hassner, editors, *European Conference on Computer Vision*, pages 1–17, 2022.
- [67] Dan Zeng, Hailin Shi, Hang Du, Jun Wang, Zhen Lei, and Tao Mei. Npcface: Negative-positive collaborative training for large-scale face recognition. 2020.
- [68] Jiaming Zhang, Qi Yi, and Jitao Sang. Towards adversarial attack on vision-language pre-training models. In *Proceedings of the 30th ACM International Conference on Multimedia*, pages 5005–5013, 2022.
- [69] Jianping Zhang, Weibin Wu, Jen-tse Huang, Yizhan Huang, Wenxuan Wang, Yuxin Su, and Michael R. Lyu. Improving adversarial transferability via neuron attribution-based attacks. In *Proceedings of the IEEE conference on computer vision and pattern recognition*, pages 14973–14982, 2022.
- [70] Yaoyao Zhong and Weihong Deng. Towards transferable adversarial attack against deep face recognition. *IEEE Transactions on Information Forensics and Security*, 16:1452–1466, 2021.
- [71] Fengfan Zhou, Hefei Ling, Yuxuan Shi, Jiazhong Chen, and Ping Li. Improving visual quality and transferability of adversarial attacks on face recognition simultaneously with adversarial restoration. In *IEEE International Conference on Acoustics, Speech and Signal Processing*, pages 4540–4544, 2024.
- [72] Fengfan Zhou, Hefei Ling, Yuxuan Shi, Jiazhong Chen, Zongyi Li, and Ping Li. Improving the transferability of adversarial attacks on face recognition with beneficial perturbation feature augmentation. *IEEE Transactions on Computational Social Systems*, pages 1–13, 2023.
- [73] Ziqi Zhou, Shengshan Hu, Minghui Li, Hangtao Zhang, Yechao Zhang, and Hai Jin. Advclip: Downstream-agnostic adversarial examples in multimodal contrastive learning. In *Proceedings of the 31st ACM International Conference on Multimedia*, pages 6311–6320, 2023.
- [74] Hegui Zhu, Yuchen Ren, Xiaoyan Sui, Lianping Yang, and Wuming Jiang. Boosting adversarial transferability via gradient relevance attack. In *IEEE/CVF International Conference on Computer Vision*, pages 4718–4727. IEEE, 2023.

A The Pseudo-code of Adversarial Pruning Attack Method

The pseudo-code of our proposed method based on the Lagrangian attack is illustrated in Algorithm 1.

Algorithm 1 Adversarial Pruning Attack Based on Lagrangian

Input: Negative face image pair $\{x^s, x^t\}$, the number of the iterations of Priming stage n , the maximum number of iterations m , maximum allowable perturbation magnitude ϵ , the surrogate FR model \mathcal{F} , the step size β and γ .

Output: An adversarial face example x_m^{adv}

```

1:  $x_0^{adv} = x^s$ 
2: for  $t = 1, \dots, n$  do
3:    $\mathcal{L}^p = \lambda \mathcal{L}^i + \mathcal{L}^d$  ▷ Priming Stage
4:    $x_t^{adv} = x_{t-1}^{adv} - \beta \text{sign} \left( \nabla_{x_{t-1}^{adv}} \mathcal{L}^p \right)$ 
5:    $x_t^{adv} = \prod_{x^s, \epsilon} (x_t^{adv})$ 
6: end for
7:  $\mathcal{I} = |x_n^{adv} - x^s|$  ▷ Pruning Stage
8:  $\mathcal{Q} = \text{Sort}(\Psi(\mathcal{I}))$ 
9:  $\mathcal{W} = \mathcal{Q}[: \kappa s]$ 
10: Get  $\mathcal{M}$  by Eq. (8).
11:  $x_n^{adv} = x^s + (x_n^{adv} - x^s) \odot \mathcal{M}$ 
12:  $\mathcal{A} = 1 - \mathcal{M}$ 
13: for  $t = n + 1, \dots, m$  do
14:    $\mathcal{L}^r = \tilde{\lambda} \mathcal{L}^i + \mathcal{L}^d$  ▷ Restoration Stage
15:    $x_t^{adv} = x_{t-1}^{adv} - \gamma \text{sign} \left( \nabla_{x_{t-1}^{adv}} \mathcal{L}^r \right)$ 
16:    $p = \mathcal{A} \odot (x_t^{adv} - x_n^{adv})$ 
17:    $x_t^{adv} = \prod_{x^s, \epsilon} (x_n^{adv} + p)$ 
18: end for

```

B The Optimization Objective of the Impersonation and Dodging Attacks

The objective of impersonation attacks in our research is to craft an adversarial example x^{adv} that causes the model \mathcal{F}^{vct} to incorrectly classify it as the target sample x^t , while simultaneously maintaining a high degree of visual similarity between x^{adv} and the original sample x^s . To be more specific, the objective can be expressed as follows:

$$\begin{aligned}
 x^{adv} &= \arg \min_{x^{adv}} (\mathcal{D}(\mathcal{F}^{vct}(x^{adv}), \mathcal{F}^{vct}(x^t))) \\
 &\text{s.t. } \|x^{adv} - x^s\|_p \leq \epsilon
 \end{aligned} \tag{13}$$

where \mathcal{D} refers to a predefined distance metric, while ϵ specifies the maximum magnitude of permissible perturbation.

In contrast, the dodging attacks introduced in this study aim to prevent the model \mathcal{F}^{vct} from correctly recognizing x^{adv} as the source sample x^s . This is achieved while maintaining a visually similar appearance between the adversarial example x^{adv} and the original input x^s . In a manner similar to impersonation attacks, the objective of dodging attacks can be formulated as follows:

$$\begin{aligned}
 x^{adv} &= \arg \max_{x^{adv}} (\mathcal{D}(\mathcal{F}^{vct}(x^{adv}), \mathcal{F}^{vct}(x^s))) \\
 &\text{s.t. } \|x^{adv} - x^s\|_p \leq \epsilon
 \end{aligned} \tag{14}$$

C The proof of the supremum of the absolute variance

In this section, we will provide the proof of the supremum of the absolute variance of the output of \mathcal{F} before and after pruning. The absolute variance can be expressed as follows:

$$\rho = \|\mathcal{F}(x + \delta) - \mathcal{F}(x)\| \quad (15)$$

where δ is the adversarial perturbation, $\|\cdot\|$ is the 2-norm.

Let us revisit an early hypothesis posited by Goodfellow et al. [14], suggesting that the linear nature of modern DNNs, resembling linear models trained on the same dataset, is the underlying cause of adversarial examples and their surprising transferability [15]. Based on the hypothesis, the FR model \mathcal{F} can be represented in the following linear form:

$$\mathcal{F}(x) = \omega x + b \quad (16)$$

where ω is the weight vector, and b is the bias term.

Hence, the absolute variance of the output of the function \mathcal{F} can be articulated as:

$$\begin{aligned} \rho &= \|\mathcal{F}(x + \delta) - \mathcal{F}(x)\| \\ &= \|\omega(x + \delta) + b - (\omega x + b)\| \\ &= \|\omega\delta\| \leq \|\omega\|\|\delta\| = \|\omega\|\mathcal{I} \end{aligned} \quad (17)$$

The supremum of the absolute variance is given by $\|\omega\|\mathcal{I}$. Within the context of gradient-based adversarial attacks, the parameters of the neural networks are typically held constant. Consequently, the vector ω can be treated as a constant. From this, we can deduce that the supremum of the absolute variance in the output of \mathcal{F} is directly proportional to the priority measure \mathcal{I} . It follows that adversarial perturbations of greater magnitude are more prioritized, as they exert a more pronounced influence on the output of the face recognition model \mathcal{F} .

D The Calculation Method of the Attack Success Rate

Due to the different objectives of the impersonation and dodging attacks, the calculation methods for the ASR also vary between the two attack types. When it comes to impersonation attacks on FR, the ASR can be computed as:

$$\text{ASR}^i = \frac{\sum_{i=1}^{N_p} \mathbb{1}(\mathcal{D}(\mathcal{F}^{vct}(x^{adv}), \mathcal{F}^{vct}(x^t)) < t^i)}{N_p} \quad (18)$$

where N_p refers to the total number of face pairs and t^i represents the impersonation attack threshold. For dodging attacks on FR systems, the ASR can be computed via the following formula:

$$\text{ASR}^d = \frac{\sum_{i=1}^{N_p} \mathbb{1}(\mathcal{D}(\mathcal{F}^{vct}(x^{adv}), \mathcal{F}^{vct}(x^s)) > t^d)}{N_p} \quad (19)$$

where the value of t^d represents the threshold for dodging attacks.

E The Calculation Method of the Multi-identity Sample Ratio

Multi-identity Sample Ratio (MSR) is the proportion of multi-identity samples that can be recognized as both the attacker and victim identities in the adversarial face examples capable of executing successful impersonation attacks. The detailed calculation method of MSR be expressed as:

$$\text{MSR} = \frac{|\mathcal{S}_1 \cap \mathcal{S}_2|}{|\mathcal{S}_2|} \quad (20)$$

where \mathcal{S}_1 and \mathcal{S}_2 are the set of the adversarial examples that are identified as the attacker and victim identities, respectively. Therefore, the \mathcal{S}_2 is the set of adversarial face examples that can perform a successful impersonation attack.

Table 4: Comparisons of ASR results (%) of dodging attack and impersonation attacks on the LFW dataset using the negative cosine similarity loss. The models in the second row are the victim models.

	ASR ^d			ASR ⁱ
	IR152	FaceNet	MF	
Baseline	2.2	16.1	99.4	25.4
Baseline + Lagrangian	4.0	26.5	100.0	26.0
Baseline + ours	8.1	39.7	100.0	26.2

Table 5: The results (%) on the LFW dataset using MF as the surrogate model. The models on the first row are the victim models.

	ASR ^d			ASR ⁱ
	IR152	FaceNet	MF	
SA	99.4	45.9	2.1	44.5
SA + Lagrangian	100.0	49.2	3.4	44.8
SA + ours	100.0	54.9	4.7	46.4

F Results on Negative Cosine Similarity Loss

Apart from the normalized L_2 distance loss (i.e. Eq. (1) and Eq. (2)), the negative cosine similarity loss is also a commonly used loss function in adversarial attacks on FR systems. In this section, we will assess the effectiveness of our proposed method regarding the negative cosine similarity loss.

For impersonation attacks, the negative cosine similarity loss can be expressed as:

$$\mathcal{L}_c^i = 1 - \cos(\mathcal{F}(x^{adv}), \mathcal{F}(x^t)) \quad (21)$$

where $\cos(e, e')$ is the function to calculate the cosine similarity between e and e' .

Similarly, the negative cosine similarity loss for dodging attacks can be formulated as follows:

$$\mathcal{L}_c^d = 1 + \cos(\mathcal{F}(x^{adv}), \mathcal{F}(x^s)) \quad (22)$$

To evaluate the effectiveness of our proposed method on the negative cosine similarity loss, we use DI as the Baseline to craft adversarial face examples using the negative cosine similarity loss \mathcal{L}_c^i and \mathcal{L}_c^d as \mathcal{L}^i and \mathcal{L}^d , respectively. The performance is demonstrated in Table 4.

Table 4 demonstrates that the performance of both impersonation and dodging improves after integrating our proposed attack method into the Baseline attack. This further highlights the effectiveness of our method regarding the negative cosine similarity loss.

G Results on Sibling-Attack

Sibling-Attack [29] (abbreviated as SA) is a cutting-edge adversarial attack on FR that demonstrates considerable effectiveness in enhancing the transferability of adversarial attacks on FR. SA employs a surrogate model with a two-branch multi-task neural network, which differs from the surrogate models discussed in Section 4.2. Consequently, we exclusively consider SA for comparison with our method.

We aligned the attack setting with the official SA implementation and integrated our proposed Adv-Pruning with SA. The FFHQ dataset, provided by the official SA page², is chosen as the dataset for generating adversarial face examples. The results are depicted in Table 5.

Table 5 demonstrates that the incorporation of our proposed method results in enhancements in both dodging and impersonation performance. This further demonstrates the effectiveness of our proposed attack method in enhancing the dodging attack performance without compromising the impersonation attack performance.

²<https://github.com/Tencent/TFace/tree/Adv-Attack-Defense/security/tasks/Adv-Attack-Defense/Sibling-Attack>

Table 6: The results (%) on the LFW dataset using MF as the surrogate model. The models on the first row are the victim models.

Attack	Metric	IR152	FaceNet	MF
DI	MSR	95.6	75.7	0.8
	ASR ^{<i>i</i>}	18.4	32.9	100.0
	ASR ^{<i>d</i>}	2.2	18.2	99.2
VMI	MSR	97.0	88.6	0.3
	ASR ^{<i>i</i>}	13.6	20.2	100.0
	ASR ^{<i>d</i>}	1.0	8.4	99.7
SSA	MSR	98.6	92.8	1.5
	ASR ^{<i>i</i>}	13.8	19.6	100.0
	ASR ^{<i>d</i>}	0.7	5.9	98.5
DFANet	MSR	98.6	96.6	0.4
	ASR ^{<i>i</i>}	7.0	11.9	100.0
	ASR ^{<i>d</i>}	0.2	1.5	99.6
SIA	MSR	97.4	83.9	1.6
	ASR ^{<i>i</i>}	15.7	26.7	100.0
	ASR ^{<i>d</i>}	1.0	10.6	98.4
BSR	MSR	98.1	96.8	15.1
	ASR ^{<i>i</i>}	5.4	9.5	100.0
	ASR ^{<i>d</i>}	0.4	3.7	84.9
BPFA	MSR	96.2	92.1	2.3
	ASR ^{<i>i</i>}	15.8	17.8	100
	ASR ^{<i>d</i>}	0.9	4.6	97.7

H Results on MSR of Previous Impersonation Attacks

Following the same experimental setting of Section 4.4, we conduct experiments on various previous impersonation attacks. The results are shown in Table 6.

As indicated by Table 6, the majority of the crafted adversarial face examples are multi-identity samples in the black-box setting. This observation suggests that the majority of adversarial face examples, which are generated through the previous impersonation attacks, fail to achieve a successful dodging attack in the black-box setting.